Lanthanide Ion Codoped Emitters for Tailoring Emission Trajectory and Temperature Sensing

Shu-Na Zhao, Lei-Jiao Li, Xue-Zhi Song, Min Zhu, Zhao-Min Hao, Xing Meng, Lan-Lan Wu, Jing Feng, Shu-Yan Song, Cheng Wang,* and Hong-Jie Zhang*

A series of lanthanide metal-organic frameworks (Ln-MOFs) are synthesized through solvothermal conditions with 1,3-bis(4-carboxyphenyl)imidazolium (H_2L). Owing to the lanthanide contraction effect, two different types of Ln-MOFs, namely, $\{[Ln(L)_2(OH)]\cdot 3H_2O\}_n$ (Ln:Pr, Nd, Sm) and $\{[Ln(L)_2(COO)(H_2O)_2]\cdot H_2O\}_n$ (Ln: Eu, Gd, Tb, Dy, Tm, Yb, Y), and their corresponding codoped Ln-MOFs $Eu_xTb_{1-x}L$ are obtained. With careful adjustment of the relative concentration of the lanthanide ions and the excitation wavelength, the color of the luminescence can be systematically modulated and white light emission can be further successfully achieved. Furthermore, by virtue of the temperature-dependent luminescent behavior, $Eu_{0.2}Tb_{0.8}L$ allows for the design of a thermometer with an excellent linear response to temperature over a wide range, from 40 to 300 K. This work highlights the practical applications of Ln-MOFs for tailoring fluorescent color and even obtaining practical white light emission, and especially for sensing temperature as luminescent thermometers in a single framework by controlling in different ways.

1. Introduction

Lanthanide luminescence attains a special status in photonics due to the unique spectroscopic features of lanthanide ions, including long lifetime, large Stokes shift, narrow band, and high color purity with respect to light generation and amplification.[1] In recent decades, the number of photonic applications of lanthanides has been burgeoning, extending from sensing to biomedical analyses, imaging, lighting and displays.[2] Moreover, the search for new lanthanide materials with controlled and tunable luminescent properties for applications in thermometry and white light emission is currently a very active field.

Temperature is a fundamental thermodynamic parameter, the measurement of which is crucial in countless scientific investigations and technological developments.[3] Among many methods for determining temperature, luminescence-based measurements have attracted more and more attention because they are noninvasive and accurate, capable of giving fast response and high spatial resolution characteristics, and able to work in even strong electro or magnetic fields and with fast-moving objects.[4] Luminescent thermometers, such as organic dyes,[5] polymers,[6] semiconductor nanocrystals,[7] and trivalent lanthanides (Ln^{3+})[8] incorporated into inorganic, organic or hybrid hosts, are generally based on the drop of their emission intensity with increasing temperature caused by the thermal activation of nonradiative deactivation pathways.[9] However, most luminescent thermometers explored until now are dependent on the luminescence intensity of single transition and are often susceptible to errors due to changes in probe concentration, excitation or detection efficiency, and are sometimes lacking specificity for temperature.[10] Such obstacles have been overcome by using ratiometric detection scheme reported by Carlos in their pioneering work on magnetic hybrid nanoparticles (NPs) codoped with Eu^{3+} and Tb^{3+} tris(β-diketonate) chelates.[8c]

Light, especially white light, one of the most important factors affects our daily lives. In general, white light emitting materials can be achieved through monochromatic, dichromatic, trichromatic, and tetrachromatic approaches.[11–13] Although a few examples of monochromatic and tertrachromatic white light emitting materials have been realized,[12] the white light emitting materials have been mainly achieved through dichromatic and trichromatic approaches in which the blue and yellow, and blue, green, and red light emitting components are incorporated into the resulting white light emitting materials, respectively.[13] To the best of our knowledge, lanthanide-doping materials are commonly used as white light emitting materials due to the controlled and fine-tuned emission trajectory. It is especially preferable for the host material with blue emission to generate white light emitting materials by introducing Eu^{3+} (red) and Tb^{3+} (green) emitters. A new approach to obtain white light emitting materials by adjusting excitation wavelength recently captures our attention not only for its broadband white emission[12b] but also for its ability to tailor colors.[11d]

Recently, the emergence of lanthanide metal-organic frameworks (Ln-MOFs) has brought promise to the development of new functional luminescent materials.[14] Such Ln-MOFs

Dr. S.-N. Zhao, L.-J. Li, X.-Z. Song, M. Zhu, Z.-M. Hao, X. Meng, L.-L. Wu, J. Feng, Prof. S.-Y. Song, Prof. C. Wang, Prof. H.-J. Zhang
CAS Key Laboratory of Rare Earth Resource Utilization
Changchun Institute of Applied Chemistry
5625 Renmin Street, Changchun 130022, P.R. China
E-mail: songsy@ciac.ac.cn; cwang@ciac.ac.cn
Dr. S.-N. Zhao, X.-Z. Song, M. Zhu, Z.-M. Hao, X. Meng, L.-L. Wu
Graduate School of the Chinese Academy of Sciences
University of Chinese Academy of Sciences
Beijing 100049, P.R. China

DOI: 10.1002/adfm.201402061

consist of central lanthanide ions and organic ligands, playing the roles of both linkers and photosensitizers.[15] Furthermore, the mutual separation of lanthanide ions by organic ligands in these materials will prevent self-quenching, and the spatial regularity of the building blocks may allow for the incorporation of different lanthanide ions into well-defined frameworks.

Taking the advantages of Ln-MOFs into consideration, we aim to modulate the emission trajectory in order to explore the applications of white light emitting materials in thermometry by controlling lanthanide ionic types and concentration, excitation wavelength. We have successfully synthesized a series of Ln-MOFs: $\{[Ln(L)_2(OH)]\cdot 3H_2O\}_n$ (Ln: Pr (**1**), Nd (**2**), Sm (**3**)); $\{[Ln(L)_2(COO)(H_2O)_2]\cdot H_2O\}_n$ (Ln: Eu (**4**), Gd (**5**), Tb (**6**), Dy (**7**), Tm (**8**), Yb (**9**), Y (**10**)) and the codoped Ln-MOFs: $Eu_xTb_{1-x}L$ (x = 0.1–0.9) with 1,3-bis(4-carboxyphenyl)imidazolium (H_2L). With judicious adjustment of the relative concentration of the lanthanide ions, the color of the luminescence can be tailored from green, through yellow to red. By changing the excitation wavelength, the emission trajectory can also be modulated to include white light emission. Furthermore, the temperature-dependent luminescent properties of $Eu_{0.2}Tb_{0.8}L$ allowed for the design of a thermometer with an excellent linear response to temperature over a wide range from 40 to 300 K.

2. Results and Discussion

2.1. Structural Characterization

Single-crystal X-ray diffraction analysis reveals that compounds **1**–**3** are isomorphic, so the crystal structure of **3** is employed as a representative example that is discussed in detail. Compound **3** crystallizes in the monoclinic space group $P2_1/n$. The asymmetric unit of compound **3** contains one crystallographically independent samarium ion, two ligands, one hydroxide ion, and two lattice water molecules. Sm^{3+} ion is eight-coordinated with a distorted bicapped trigonal prismatic geometry by eight oxygen atoms from one chelating carboxylic group (O1, O2), five dimonodentate carboxylic groups (O2A, O3B, O6, O7C, and O8D), and one hydroxide ion (O9) (**Figure 1**). The Sm–O (carboxylate) bond distances range from 2.275(6) to 2.562(6) Å, which are comparable to those reported for other Sm–O donor compounds.[16] As shown in Figure S1a (Supporting Information), two crystallographically equivalent Sm atoms are bridged by two ligands to form a binuclear building block, which were further connected with each other through two carboxylic groups along the *a* direction. This leads to the formation of a 1D infinite chain, –Sm–O–C–O–Sm–, as reported in other lanthanide MOFs[17] (the adjacent Sm···Sm separation is 4.1301 Å). The Sm atoms of the adjacent 1D chains are connected by ligands to form the wavy 2D layer framework (Figure S1c, Supporting Information). Along the *b* direction, adjacent 2D layers are packed parallel in a ...ABAB... fashion to generate an intricate 3D network via van der Waals forces (Figure S1b, Supporting Information).

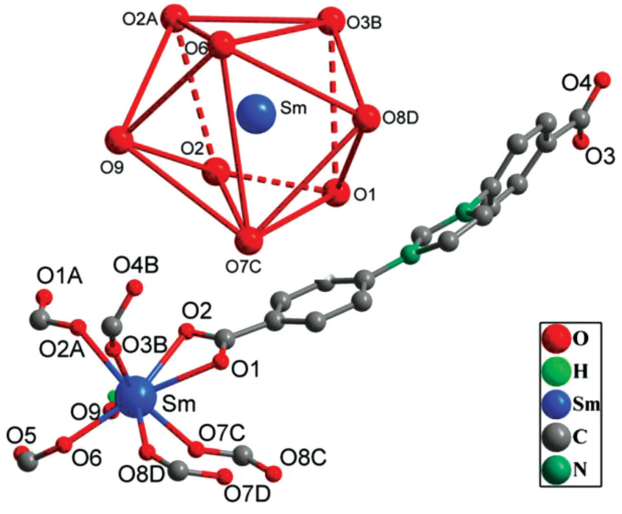

Figure 1. View of the eight-coordinated Sm^{3+} ion with a distorted bicapped trigonal prismatic geometry. Symmetry codes: A, -*x*, -*y*, 1-*z*; B, *x*, *y*, 1-*z*; C, *x*, *y*, 1+*z*; D, 1-*x*, -*y*, -*z*.

When other the lanthanide ions (Eu^{3+}, Gd^{3+}, Tb^{3+}, Dy^{3+}, Tm^{3+}, Yb^{3+}, and Y^{3+}) are used instead, another type of isosturctural framework was obtained. The crystal structure of compound **4** is presented as a representative example of these compounds. Compound **4** crystallizes in the triclinic system, space group $P\bar{1}$ and features a one-dimensional chain based on Eu^{3+} ions and ligands. The asymmetric unit of **4** consists of one crystallographically independent Eu^{3+} ion, two ligands, two aqua ligands, and one formate ion. Each Eu^{3+} center is coordinated with seven oxygen atoms, including four dimonodentate carboxylic oxygen atoms from four ligands (O1, O4B, O5, and O8A) and one formate ion (O9), and two oxygen atoms from two aqua ligands (O10 and O12) (**Figure 2**a). Therefore, the coordination geometry around the metal center can be appropriately described as a distorted monocapped trigonal prism. The Eu–O distances vary from 2.303(3) to 2.453(2) Å, in accordance with the reported values for other europium-carboxylic oxygen donor compounds.[18] The adjacent Eu^{3+} centers are linked via two ligands to form an infinite wavy double-chain along the *b* direction, as shown in Figure 2b. These chains pile up into a 3D network through van der Waals forces and hydrogen-bond interactions (Figure 2c).

Importantly, compounds **1**–**10** were obtained under identical synthetic conditions, demonstrating that the structural differences provide profound insights into the vital influence of lanthanide contraction. The isostructural framework of Eu and Tb would afford us the opportunity to prosperously synthesize codoped Ln-MOFs that exhibit fine-tuned emission trajectory for color tailoring and temperature sensing.

2.2. Photoluminescent Properties

The luminescent properties of solid-state lighting applications are very interesting, especially when the ligands themselves display luminescence within these materials. The excitation and emission spectra of ligand and the corresponding lanthanide compounds in the solid state were investigated at room temperature. As shown in Figure S4 (Supporting Information), the free H_2L ligand shows a broad emission band with a maximum at 435 nm (λ_{ex} = 347 nm), which is attributed to a π^*–π transition. Upon excitation

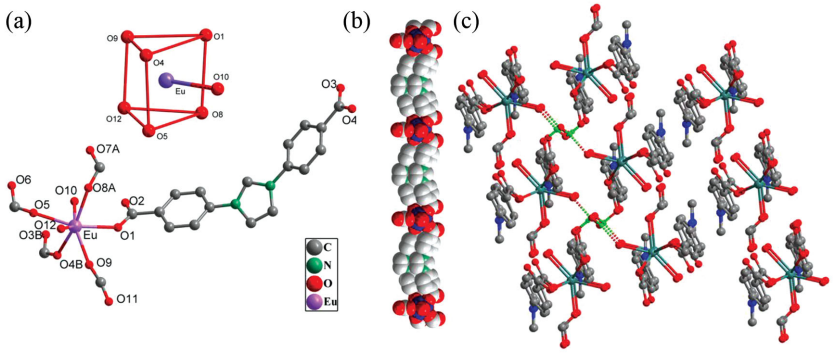

Figure 2. a) View of the seven-coordinated Eu^{3+} ion with a monocapped trigonal prismatic geometry. Symmetry codes: A, 1+*x*, −1+*y*, *z*; B, −1+*x*, 1+*y*, *z*. b) The 1D metal chain extending along *a* direction. c) The 3D framework of compound **4** constructed by the 1D chain via van der Waals force and hydrogen-bonding interactions.

at 320 nm, compound **4** possesses four major peaks assigned to the $^5D_0 \rightarrow {}^7F_J$ (J = 1–4) transitions, which are $^5D_0 \rightarrow {}^7F_1$ (591 nm), $^5D_0 \rightarrow {}^7F_2$ (615 nm), $^5D_0 \rightarrow {}^7F_3$ (650 nm), and $^5D_0 \rightarrow {}^7F_4$ (698 nm) (Figure S5, Supporting Information). However, the persistent presence of ligand-originated emission in the luminescence spectrum of compound **4** signifies that the efficiency of energy transfer from the ligand to the Eu^{3+} ion is not thorough. Compound **6** exhibits four typical emissions excited at 320 nm, which are assigned to the $^5D_4 \rightarrow {}^7F_J$ (J = 3–6), $^5D_4 \rightarrow {}^7F_6$ (488 nm), $^5D_4 \rightarrow {}^7F_5$ (541 nm), $^5D_4 \rightarrow {}^7F_4$ (583 nm), and $^5D_4 \rightarrow {}^7F_3$ (618 nm) transitions (Figure S6, Supporting Information). Notably, the strong blue emission in free ligand completely disappears, revealing that H_2L ligand is an excellent chromophore for sensitization of the Tb^{3+}ion.

Comparison of the emission spectra of compounds **4** and **6** demonstrates that the transition intensity follows the trend of $Tb^{3+} >> Eu^{3+}$, originating from higher energy transfer efficiency from the organic ligands to Tb^{3+} than to Eu^{3+}. Investigation into the luminescence lifetime further proves these results. The relatively short lifetime (0.35 ms) of the Eu^{3+} compound indicates that the Eu^{3+} ions is poorly sensitized, whereas the Tb^{3+} ions (0.79 ms) is preferably sensitized.

2.3. Fine-Tuned Emission Trajectory Properties

Due to the isostructural compounds **4** and **6**, we expected that the emissions could be easily tuned by using a doping method. As shown in **Figure 3**a, the emission spectra of the codoped MOF $Eu_xTb_{1-x}L$ (x = 0.1–0.9) with different doping concentrations exhibit characteristic transitions of both Eu^{3+} and Tb^{3+} ions. Along with the increase of Eu^{3+} concentration, the luminescence intensity of the Tb^{3+} ion gradually decreases while the luminescence intensity of the Eu^{3+} ion increases. Therefore, the luminescent colors of the codoped MOF $Eu_xTb_{1-x}L$ (x = 0.1–0.9) can be tuned from green to green-yellow, yellow, orange, red-orange, and red. The corresponding 1931 CIE chromaticity coordinates can be changed from (0.309, 0.583) to (0.596, 0.313) by changing the doping concentration of the Eu^{3+} ion (Figure 3b).

Surprisingly, when the excitation wavelength of codoped MOF $Eu_{0.25}Tb_{0.75}L$ was controlled from 330 to 395 nm, the color footprints across the yellow, green-yellow, and especially white light emission regions were found. The emission spectra of codoped MOF $Eu_{0.25}Tb_{0.75}L$ essentially display the typical $^5D_0 \rightarrow {}^7F_J$ (J = 1–4) transitions and the broad ligand-based band for compound **4** as well as the $^5D_4 \rightarrow {}^7F_J$ (J = 3–6) transitions for compound **6** (**Figure 4**a). This finding reveals that the relative blue, red, and green emission intensities can be tuned by varying the excitation wavelength. As a consequence, white light emission can be indeed achieved when the compound is excited at 380, 385, 390, 395 nm, with the corresponding CIE coordinates of (0.323, 0.358), (0.323, 0.337), (0.314, 0.327), and (0.339, 0.323), respectively (Figure 4b). All are very close to the coordinate for pure white light (0.333, 0.333), thus ideal for the white light emission according to the CIE coordinate diagram.

This interesting observation of codoped MOF $Eu_{0.25}Tb_{0.75}L$ inspired us to further investigate the emission spectra of other

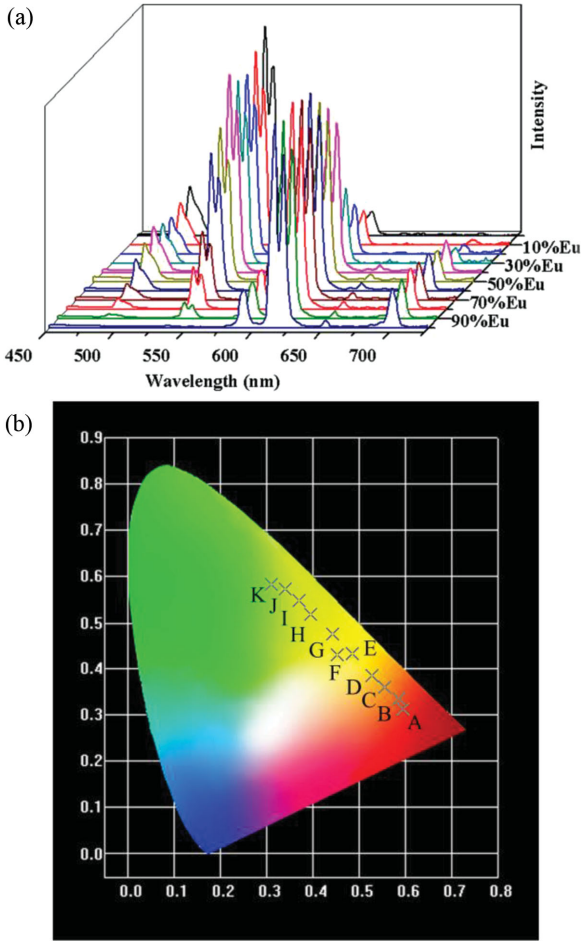

Figure 3. a) The emission spectra of the codoped MOF $Eu_xTb_{1-x}L$ (λ_{ex} = 320 nm). b) CIE chromaticity diagram for $Eu_xTb_{1-x}L$ (A → K, increasing the concentration of Eu^{3+} ion).

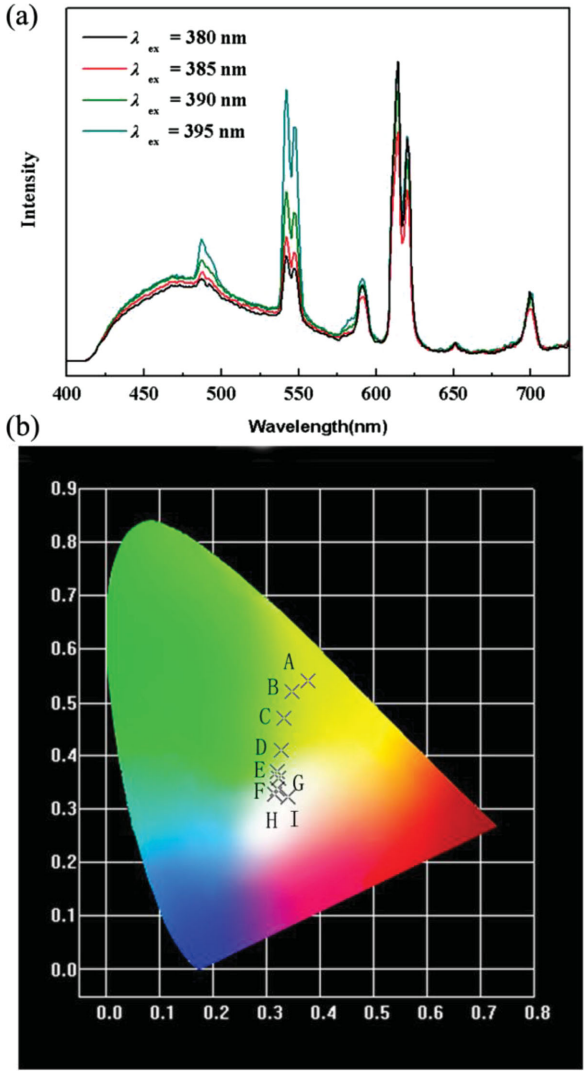

Figure 4. a) Room-temperature emission spectra for the $Eu_{0.25}Tb_{0.75}L$ in the solid state excited at 380, 385, 390, 395 nm. b) CIE chromaticity diagram for $Eu_{0.25}Tb_{0.75}L$ (A → I, increasing the excitation wavelength from 330 to 395 nm).

codoped MOFs. A similar color trajectory was also realized in other codoped MOF $Eu_xTb_{1-x}L$ (x = 0.2, 0.28, 0.3) compounds, all of which contain white light emission (Figures S9–S11, Supporting Information). It develops a potential approach for managing white light emission by using these codoped MOFs $Eu_xTb_{1-x}L$ (x = 0.2, 0.25, 0.28, 0.3).

2.4. Temperature-Dependent Photoluminescent Properties

Codoped MOF $Eu_xTb_{1-x}L$ compounds also feature fascinating temperature-dependent luminescence, which enables them excellent candidates for self-referencing luminescent thermometers.[8c,19] We have investigated both the intensity and lifetime of the codoped MOF $Eu_xTb_{1-x}L$ to illustrate their potential application as luminescent thermometers. The temperature-dependent emission spectra of compounds **4**, **6**, and codoped MOF $Eu_{0.2}Tb_{0.8}L$ from 40 to 300 K are shown in **Figures 5**a,b and **6**a. The integrated intensities of $^5D_4 \rightarrow {}^7F_5$ (Tb^{3+}, 543 nm) and $^5D_0 \rightarrow {}^7F_2$ (Eu^{3+}, 616 nm) are portrayed in Figures 5c and 6b. The luminescent intensities of both Tb^{3+} and Eu^{3+} ions in compounds **4** and **6** decrease gradually with increasing temperature, which is normal due to the thermal activation of nonradiative-decay pathways.[9] However, the codoped MOF $Eu_{0.2}Tb_{0.8}L$ exhibits a significantly different temperature-dependent luminescent behavior with respect to the emissions of Tb^{3+} ions at 543 nm and Eu^{3+} ions at 615 nm. The emission intensity of the Tb^{3+} ions decreases as the temperature increases, while that of the Eu^{3+} ions increases. To the best of our knowledge, the intensity ratio of two emissions is commonly used as the thermometric parameter in ratiometric luminescence temperature sensing. For the codoped MOF $Eu_{0.2}Tb_{0.8}L$, this parameter can be defined by using the ratio of the intensity of the $^5D_4 \rightarrow {}^7F_5$ (Tb^{3+}, 543 nm) and $^5D_0 \rightarrow {}^7F_2$ (Eu^{3+}, 615 nm) transitions (I_{Tb}/I_{Eu}), which does not require any additional calibration of the luminescence intensity. The temperature-dependence of the I_{Tb}/I_{Eu} ratio is depicted in Figure 6c. The good linear relationship between the I_{Tb}/I_{Eu} ratio and temperature from 40 to 300 K can be fitted as a function of

$$T = 948.81 - 169.49 I_{Tb}/I_{Eu} \quad (1)$$

with a correlation coefficient of 0.9932, which demonstrates that $Eu_{0.2}Tb_{0.8}L$ is an excellent luminescent thermometer at this temperature range.

We have also investigated other codoped MOFs $Eu_xTb_{1-x}L$ (x = 0.1, 0.3, 0.4). Similar results were also observed in $Eu_{0.3}Tb_{0.7}L$, but other codoped MOFs exhibited strongly decreasing Tb^{3+}emission intensities and slightly decreasing Eu^{3+} emission intensities (Figures S13–S15, Supporting Information). Both $Eu_{0.1}Tb_{0.9}L$ and $Eu_{0.3}Tb_{0.7}L$ showed good linear relationships between the I_{Tb}/I_{Eu} ratio and temperatures ranging from 40 to 300 K with the functions T = 1180.99–140.85I_{Tb}/I_{Eu} and T = 889.52–238.10I_{Tb}/I_{Eu}, respectively. Compared with the codoped MOF $Eu_xTb_{1-x}L$ (x = 0.1, 0.2, 0.3), the relative sensitivity increases slightly from 40 to 300 K, and all gets their maximum values of 0.11%/K, 0.15%/K, and 0.17%/K at 300 K.[20] (Figure S17, Supporting Information) Although the $Eu_{0.3}Tb_{0.7}L$ shows highest maximum relative sensitivity, the $Eu_{0.2}Tb_{0.8}L$ has a corrected parameter that is more perfectly linear, which makes this material a more reliable and useful luminescent thermometer. A series of related work reported by other groups[21] has also summarized for the further study of the potential applications of $Eu_{0.2}Tb_{0.8}L$. It is clear that $Eu_{0.2}Tb_{0.8}L$ displays a linear response from cryogenic temperature up to room temperature (Table S3, Supporting Information). Although $Eu_{0.2}Tb_{0.8}L$ is deficient in relative sensitivity, it still has more application prospect in scientific and industrial fields over a wide temperature range.

The remarkable temperature-dependent emissions may be explained by the probability of temperature-dependent energy transfer from the Tb^{3+} to Eu^{3+} ions. To better understand the mechanism of energy transfer, the lifetimes of the excited states $^5D_0$ (Eu^{3+}) and $^5D_4$ (Tb^{3+}) at different temperatures within these luminescent MOFs were monitored at 615 and 543 nm, respectively (Figure 5d). The lifetimes of

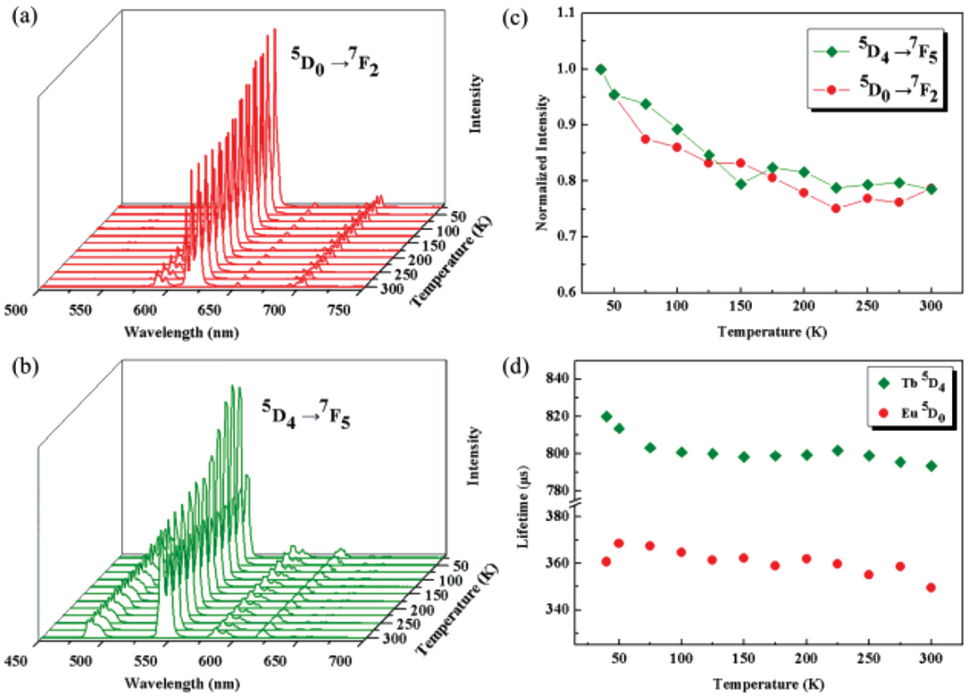

Figure 5. Emission spectra of a) **6** (TbL) and b) **4** (EuL) recorded between 40 and 300 K (excited at 322 nm). c) Temperature-dependent intensity of the $^5D_4 \rightarrow ^7F_5$ transition of **6** (TbL) and $^5D_0 \rightarrow ^7F_2$ transition of **4** (EuL), and d) temperature dependence of the $^5D_4$ lifetime for **6** (TbL) and $^5D_0$ lifetime for **4** (EuL). Decay curves are monitored at 543 and 615 nm, respectively, and excited at 322 nm.

$^5D_0$ in **4** and $^5D_4$ in **6** decreased by approximately 5% as the temperature was increased from 40 to 300 K, while the lifetime of $^5D_0$ in $Eu_{0.2}Tb_{0.8}L$ increased by approximately 13%. (Figure 6d) In fact, $Eu_{0.2}Tb_{0.8}L$ possesses a shorter $^5D_4$ (Tb^{3+}) lifetime than that of **6** but a longer $^5D_0$ (Eu^{3+}) lifetime than that of **4** at the same temperature. These phenomena indicate that energy transfer from the Tb^{3+} to Eu^{3+} ions does occur. In theory, the efficiency of energy transfer (E) between the donor

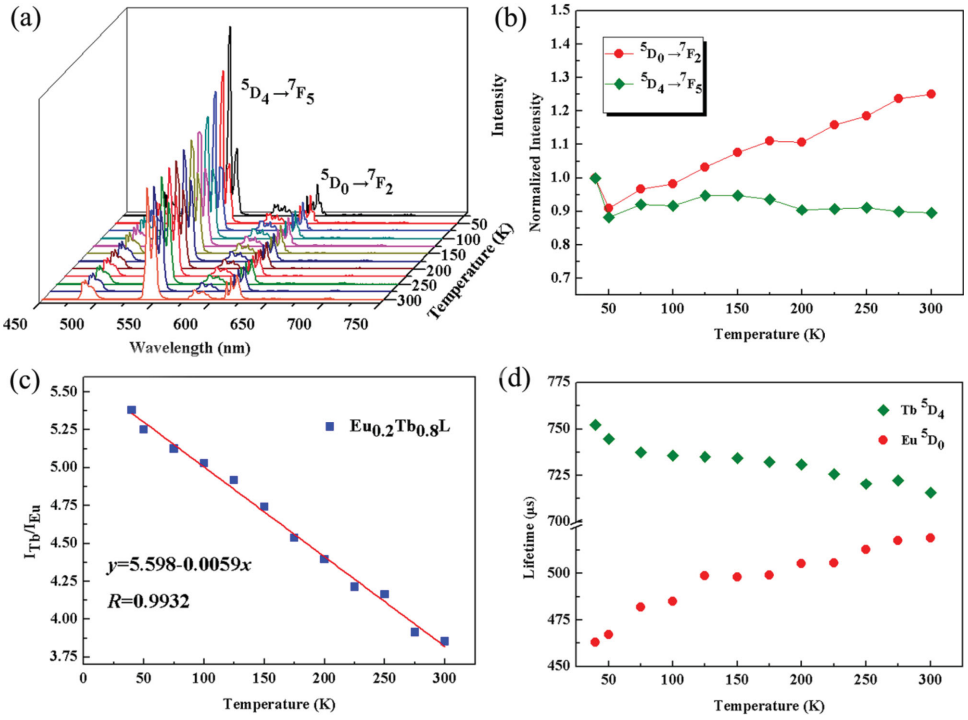

Figure 6. a) Emission spectra of $Eu_{0.2}Tb_{0.8}L$ recorded between 40 and 300 K (excited at 322 nm); b) temperature-dependent intensity of the $^5D_4 \rightarrow ^7F_5$ and $^5D_0 \rightarrow ^7F_2$ transition for $Eu_{0.2}Tb_{0.8}L$; c) temperature-dependent intensity ratio of Tb^{3+} (543 nm) to Eu^{3+} (615 nm); d) temperature dependence of the $^5D_4$ lifetime for **6** (TbL) and $^5D_0$ lifetime for **4** (EuL). Decay curves are monitored at 543 and 615 nm, respectively, and excited at 322 nm.

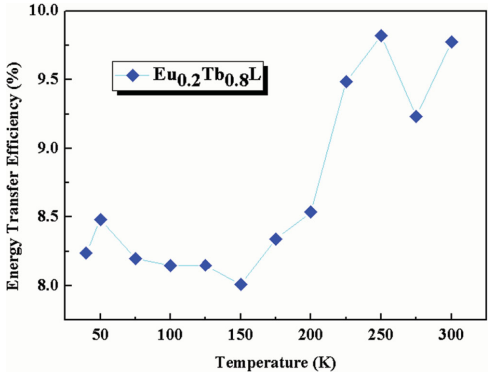

Figure 7. Temperature dependence of the energy transfer efficiency from Tb^{3+} to Eu^{3+} in $Eu_{0.2}Tb_{0.8}L$

and acceptor can be calculated from the lifetime of donor luminescence:[22]

$$E = 1 - \tau_{da}/\tau_{d} \quad (2)$$

where τ_{da} and τ_{d} are the donor's excited-state lifetime in the presence and absence of the acceptor, respectively. As shown in **Figure 7**, the energy transfer efficiency from Tb^{3+} to Eu^{3+} ions is weak at the cryogenic region and strongly enhanced at the elevated temperature, which might be mainly controlled by the phonon-assisted Förster transfer mechanism.[23]

3. Conclusion

In summary, a series of novel Ln-MOFs have been successfully synthesized under solvothermal conditions. The emission trajectory of codoped Ln-MOFs can be exquisitely tuned by controlling the lanthanide types, careful optimization their concentration, and their excitation wavelength. By changing the ratio of Eu^{3+} and Tb^{3+}, the color can be tailored from green to red. By increasing the excitation wavelength, we also found that color change could be controlled to attain white light emission. Furthermore, the codoped MOF $Eu_{0.2}Tb_{0.8}L$ can be applied as a luminescent thermometer due to its excellent linear correlation between temperature and luminescence intensity ratio from 40 to 300 K. We believe that the codoped approach opens up a new perspective for the development of white light emitting materials and temperature sensors. There are still many challenges to exploring white light emitting materials with high performance and temperature sensors with higher sensitivity over a wide temperature range that we will strive to work on in the future.

4. Experimental Section

Synthesis of $\{[Pr(L)_2(OH)]\cdot 3H_2O\}_n$ ***(1)***: A mixture containing H_2L (0.0259 g, 0.075 mmol), $Pr(NO_3)_3\cdot 6H_2O$ (0.0218 g, 0.05 mmol) in 3 mL of DMF and 1.5 mL of H_2O solution was sealed in a Teflon-lined autoclave and heated at 120 °C under autogenous pressure for three days and then allowed to cool to room temperature. The crystals were washed with water and air-dried. Yield: 65% (based on Pr^{3+}). Anal. Calcd for $C_{34}H_{29}N_4O_{12}Pr$ (Mr: 826.52): C, 49.40; H, 3.54; N, 6.78. Found: C, 50.07; H, 3.35; N, 6.52.

Synthesis of $\{[Nd(L)_2(OH)]\cdot 3H_2O\}_n$ ***(2)***: Yield: 58% (based on Nd^{3+}). Anal. Calcd for $C_{34}H_{29}N_4O_{12}Nd$ (Mr: 829.85): C, 49.21; H, 3.54; N, 6.75. Found: C, 49.07; H, 3.82; N, 6.37.

Synthesis of $\{[Sm(L)_2(OH)]\cdot 3H_2O\}_n$ ***(3)***: Yield: 44% (based on Sm^{3+}). Anal. Calcd for $C_{34}H_{29}N_4O_{12}Sm$ (Mr: 835.96): C, 48.85; H, 3.50; N, 6.70. Found: C, 49.23; H, 3.17; N, 6.45.

Synthesis of $\{[Eu(L)_2(COO)(H_2O)_2]\cdot H_2O\}_n$ ***(4)***: A mixture containing H_2L (0.0259 g, 0.075 mmol), $Eu(NO_3)_3\cdot 6H_2O$ (0.0223 g, 0.05 mmol) in 3 mL of DMF and 1.5 mL of H_2O solution was sealed in a Teflon-lined autoclave and heated at 120 °C under autogenous pressure for three days and then allowed to cool to room temperature. The crystals were washed with water and air-dried. Yield: 45% (based on Eu^{3+}). Anal. Calcd for $C_{35}H_{28}N_4O_{13}Eu$ (Mr: 864.59): C, 48.62; H, 3.26; N, 6.48. Found: C, 48.16; H, 3.32; N, 6.61.

Synthesis of $\{[Gd(L)_2(COO)(H_2O)_2]\cdot H_2O\}_n$ ***(5)***: Yield: 52% (based on Gd^{3+}). Anal. Calcd for $C_{35}H_{28}N_4O_{13}Gd$ (Mr: 869.86): C, 48.33; H, 3.24; N, 6.44. Found: C, 48.67; H, 3.68; N, 5.94.

Synthesis of $\{[Tb(L)_2(COO)(H_2O)_2]\cdot H_2O\}_n$ ***(6)***: Yield: 48% (based on Tb^{3+}). Anal. Calcd for $C_{35}H_{28}N_4O_{13}Tb$ (Mr: 871.53): C, 48.24; H, 3.24; N, 6.43. Found: C, 48.01; H, 3.87; N, 6.21.

Synthesis of $\{[Dy(L)_2(COO)(H_2O)_2]\cdot H_2O\}_n$ ***(7)***: Yield: 56% (based on Dy^{3+}). Anal. Calcd for $C_{35}H_{28}N_4O_{13}Dy$ (Mr: 875.11): C, 48.04; H, 3.22; N, 6.40. Found: C, 48.53; H, 3.07; N, 5.95.

Synthesis of $\{[Tm(L)_2(COO)(H_2O)_2]\cdot H_2O\}_n$ ***(8)***: Yield: 40% (based on Tm^{3+}). Anal. Calcd for $C_{35}H_{28}N_4O_{13}Tm$ (Mr: 881.54): C, 47.69; H, 3.20; N, 6.36. Found: C, 48.09; H, 3.54; N, 6.15.

Synthesis of $\{[Yb(L)_2(COO)(H_2O)_2]\cdot H_2O\}_n$ ***(9)***: Yield: 43% (based on Yb^{3+}). Anal. Calcd for $C_{35}H_{28}N_4O_{13}Yb$ (Mr: 885.65): C, 47.47; H, 3.19; N, 6.33. Found: C, 47.14; H, 3.03; N, 6.79.

Synthesis of $\{[Y(L)_2(COO)(H_2O)_2]\cdot H_2O\}_n$ ***(10)***: Yield: 43% (based on Y^{3+}). Anal. Calcd for $C_{35}H_{28}N_4O_{13}Y$ (Mr: 801.52): C, 47.47; H, 3.19; N, 6.33. Found: C, 47.14; H, 3.03; N, 6.79.

Synthesis of Ln-Doped Analogies: $Eu_xTb_{1-x}L$: Typically, a mixture of $Eu(NO_3)_3\cdot 6H_2O$ aqueous (0.1 mol L^{-1}, *a* mL), $Tb(NO_3)_3\cdot 6H_2O$ aqueous (0.1 mol L^{-1}, *b* mL), H_2L (0.075 mmol), DMF (3.0 mL), and H_2O (1.5-*a*-*b* mL), was added to a 15 mL Teflon-lined stainless-steel autoclave and heated at 120 °C for 3 days. After it was cooled to room temperature, colorless crystalline-like powder were collected, washed with water and air-dried. (The volume *a*, *b*, of $Ln(NO_3)_3\cdot 6H_2O$ was calculated from the corresponding doping concentration *x*, *y*).

Crystal Data: **3** $C_{34}H_{29}N_4O_{12}Sm$, M_r = 835.96, monoclinic, $P2_1/n$, a = 8.9080(5), b = 20.5433(12), c = 17.0668(10), β = 97.8900(10)°, V = 3093.7(3) Å^3, Z = 4, D_c = 1.795 g cm^{-3}, reflections collected/independent: 17507/5484, R_{int} = 0.0764. The final R_1 = 0.0443 ($I > \sigma(I)$), wR_2 = 0.1114 (all data), GOF = 1.007. **4**: $C_{35}H_{28}N_4O_{13}Eu$, M_r = 864.57, triclinic, $P\bar{1}$, a = 11.0490(14), b = 11.2137(15), c = 15.025(2), α = 103.865(2)°, β = 90.9390(10)°, γ = 108.052(2)°, V = 1673.8(4) Å^3, Z = 2, D_c = 1.715 g cm^{-3}, reflections collected/independent: 9322/6528, R_{int} = 0.108.The final R_1 = 0.0281 ($I > \sigma(I)$), wR_2 = 0.0575 (all data), GOF = 1.087. The crystal data of other compounds are shown in Table S1 (Supporting Information). CCDC 994699–994708 contain the supplementary crystallographic data for this paper. These data can be obtained free of charge from The Cambridge Crystallographic Data Centre via www.ccdc.cam.ac.uk/data_request/cif.

Supporting Information

Supporting Information is available from the Wiley Online Library or from the author.

Acknowledgements

The authors are grateful for the financial aid from the National Natural Science Foundation of China (Grant Nos. 21221061, 51372242, 91122030, and 21210001), the National Key Basic Research Program of

China (Grant No. 2014CB643802), and Jilin Province Youth Foundation (Grant No. 20130522122JH).

Received: June 21, 2014
Revised: December 20, 2014
Published online: January 27, 2015

[1] a) J.-C. G. Bünzli, C. Piguet, *Chem. Soc. Rev.* **2005**, *34*, 1048; b) Y. Cui, Y. Yue, G. Qian, B. Chen, *Chem. Rev.* **2012**, *112*, 1126; c) R. Hao, M. Li, Y. Wang, J. Zhang, Y. Ma, L. Fu, X. Wen, Y. Wu, X. Ai, S. Zhang, Y. Wei, *Adv. Funct. Mater.* **2007**, *17*, 3663; d) L. Meyer, F. Schönfeld, K. Müller-Buschbaum, *Chem. Commun.* **2014**, *50*, 8093; e) Y. Zhang, X. Li, D. Geng, M. Shang, H. Lian, Z. Cheng, J. Lin, *CrystEngComm* **2014**, *16*, 2196; f) Y. Zhang, D. Geng, M. Shang, X. Zhang, X. Li, Z. Cheng, H. Lian, J. Lin, *Dalton Trans.* **2013**, *42*, 4799.

[2] a) J.-C. G. Bünzli, *Chem. Rev.* **2010**, *110*, 2729; b) K. Binnemans, *Chem. Rev.* **2009**, *109*, 4283; c) J.-C. G. Bünzli, S. V. Eliseeva, *Chem. Sci.* **2013**, *4*, 1939; d) P. Wu, J. Wang, C. He, X. Zhang, Y. Wang, T. Liu, C. Duan, *Adv. Funct. Mater.* **2012**, *22*, 1698; e) M. Tropiano, S. Faulkner, *Chem. Commun.* **2014**, *50*, 4696; f) J. C. Rybak, M. Hailmann, P. R. Matthes, A. Zurawski, J. Nitsch, A. Steffen, J. G. Heck, C. Feldmann, S. Gotzendorfer, J. Meinhardt, G. Sextl, H. Kohlmann, S. J. Sedlmaier, W. Schnick, K. Muller-Buschbaum, *J. Am. Chem. Soc.* **2013**, *135*, 6896; g) P. Zhou, D. Zhou, L. Tao, Y. Zhu, W. Xu, S. Xu, S. Cui, L. Xu, H. Song, *Light Sci. Appl.* **2014**, *3*, e209.

[3] a) P. R. N. Childs, J. R. Greenwood, C. A. Long, *Rev. Sci. Instrum.* **2000**, *71*, 2959; b) J. Seyedyagoobi, *Rev. Sci. Instrum.* **1991**, *62*, 249; c) J. Feng, L. Xiong, S. Wang, S. Li, Y. Li, G. Yang, *Adv. Funct. Mater.* **2013**, *23*, 340.

[4] a) C. D. S. Brites, P. P. Lima, N. J. O. Silva, A. Millán, V. S. Amaral, F. Palacio, L. D. Carlos, *New J. Chem.* **2011**, *35*, 1177; b) J. Feng, K. Tian, D. Hu, S. Wang, S. Li, Y. Zeng, Y. Li, G. Yang, *Angew. Chem.* **2011**, *123*, 8222; *Angew. Chem., Int. Ed.* **2011**, *50*, 8072; c) L. D. Carlos, R. A. Ferreira, V. de Zea Bermudez, B. Julian-Lopez, P. Escribano, *Chem. Soc. Rev.* **2011**, *40*, 536.

[5] a) P. Low, B. Kim, N. Takama, C. Bergaud, *Small* **2008**, *4*, 908; b) N. Chandrasekharan, L. A. Kelly, *J. Am. Chem. Soc.* **2001**, *123*, 9898.

[6] a) C. Gota, K. Okabe, T. Funatsu, Y. Harada, S. Uchiyama, *J. Am. Chem. Soc.* **2009**, *131*, 2766; b) E. M. Graham, K. Iwai, S. Uchiyama, A. P. de Silva, S. W. Magennis, A. C. Jones, *Lab Chip* **2010**, *10*, 1267.

[7] a) V. A. Vlaskin, N. Janssen, J. van Rijssel, R. Beaulac, D. R. Gamelin, *Nano Lett.* **2010**, *10*, 3670; b) G. W. Walker, V. C. Sundar, C. M. Rudzinski, A. W. Wun, M. G. Bawendi, D. G. Nocera, *Appl. Phys. Lett.* **2003**, *83*, 3555.

[8] a) M. Mitsuishi, S. Kikuchi, T. Miyashita, Y. Amao, *J. Mater. Chem.* **2003**, *13*, 2875; b) H. Peng, M. I. Stich, J. Yu, L. N. Sun, L. H. Fischer, O. S. Wolfbeis, *Adv. Mater.* **2010**, *22*, 716; c) C. D. Brites, P. P. Lima, N. J. Silva, A. Millan, V. S. Amaral, F. Palacio, L. D. Carlos, *Adv. Mater.* **2010**, *22*, 4499.

[9] H. Peng, M. I. Stich, J. Yu, L. N. Sun, L. H. Fischer, O. S. Wolfbeis, *Adv. Mater.* **2010**, *22*, 716; b) M. L. Bhaumik, *J. Chem. Phys.* **1964**, *40*, 3711.

[10] M. I. Stich, L. H. Fischer, O. S. Wolfbeis, *Chem. Soc. Rev.* **2010**, *39*, 3102.

[11] a) M. L. Ma, C. Ji, S. Q. Zang, *Dalton Trans.* **2013**, *42*, 10579; b) A. Ablet, S. M. Li, W. Cao, X. J. Zheng, W. T. Wong, L. P. Jin, *Chem. Asian J.* **2013**, *8*, 95; c) X. Rao, Q. Huang, X. Yang, Y. Cui, Y. Yang, C. Wu, B. Chen, G. Qian, *J. Mater. Chem.* **2012**, *22*, 3210; d) M.-S. Wang, S.-P. Guo, Y. Li, L.-Z. Cai, J.-P. Zou, G. Xu, W.-W. Zhou, F.-K. Zheng, G.-C. Guo, *J. Am. Chem. Soc.* **2009**, *131*, 13572; e) J. Hye Oh, S. Ji Yang, Y. Rag Do, *Light Sci. Appl.* **2014**, *3*, e141; f) J. He, M. Zeller, A. D. Hunter, Z. Xu, *J. Am. Chem. Soc.* **2012**, *134*, 1553.

[12] a) Y. H. Zhang, X. Li, S. Song, *Chem. Commun.* **2013**, *49*, 10397; b) D. F. Sava, L. E. Rohwer, M. A. Rodriguez, T. M. Nenoff, *J. Am. Chem. Soc.* **2012**, *134*, 3983; c) X. Li, J. D. Budai, F. Liu, J. Y. Howe, J. Zhang, X.-J. Wang, Z. Gu, C. Sun, R. S. Meltzer, Z. Pan, *Light Sci. Appl.* **2013**, *2*, e50; d) C. Xiang, W. Koo, F. So, H. Sasabe, J. Kido, *Light Sci. Appl.* **2013**, *2*, e74.

[13] a) Y. Wei, Q. Li, R. Sa, K. Wu, *Chem. Commun.* **2014**, *50*, 1820; b) M. Zhu, Z. M. Hao, X. Z. Song, X. Meng, S. N. Zhao, S. Y. Song, H. J. Zhang, *Chem. Commun.* **2014**, *50*, 1912; c) X. Ma, X. Li, Y.-E. Cha, L.-P. Jin, *Cryst. Growth Des.* **2012**, *12*, 5227; d) C. Y. Sun, X. L. Wang, X. Zhang, C. Qin, P. Li, Z. M. Su, D. X. Zhu, G. G. Shan, K. Z. Shao, H. Wu, J. Li, *Nat. Commun.* **2013**, *4*, 2717; e) Q. Tang, S. Liu, Y. Liu, D. He, J. Miao, X. Wang, Y. Ji, Z. Zheng, *Inorg. Chem.* **2014**, *53*, 289.

[14] a) P. Falcaro, S. Furukawa, *Angew. Chem.* **2012**, *124*, 8557; *Angew. Chem., Int. Ed.* **2012**, *51*, 8431; b) R. F. D'Vries, S. Álvarez-García, N. Snejko, L. E. Bausá, E. Gutiérrez-Puebla, A. de Andrés, M. Á. Monge, *J. Mater. Chem. C* **2013**, *1*, 6316; c) S. Zhang, D. Du, K. Tan, J. Qin, H. Dong, S. Li, W. He, Y. Lan, P. Shen, Z. Su, *Chem.-Eur. J.* **2013**, *19*, 11279; d) H. Zhang, X. Shan, Z. Ma, L. Zhou, M. Zhang, P. Lin, S. Hu, E. Ma, R. Li, S. Du, *J. Mater. Chem. C* **2014**, *2*, 1367; e) L. He, Y. Liu, J. Liu, Y. Xiong, J. Zheng, Y. Liu, Z. Tang, *Angew. Chem.* **2013**, *125*, 3829; *Angew. Chem., Int. Ed.* **2013**, *52*, 3741.

[15] a) N. Wartenberg, O. Raccurt, E. Bourgeat-Lami, D. Imbert, M. Mazzanti, *Chem. - Eur. J.* **2013**, *19*, 3477; b) Y. Wang, J. Yang, Y. Y. Liu, J. F. Ma, *Chem. - Eur. J.* **2013**, *19*, 14591; c) E. J. New, A. Congreve, D. Parker, *Chem. Sci.* **2010**, *1*, 111.

[16] a) Z.-P. Deng, L.-H. Huo, H.-Y. Wang, S. Gao, H. Zhao, *CrystEngComm* **2010**, *12*, 1526; b) G. Qi, Y. Lin, J. Hu, *Polyhedron* **1995**, *14*, 413.

[17] S. Su, W. Chen, C. Qin, S. Song, Z. Guo, G. Li, X. Song, M. Zhu, S. Wang, Z. Hao, H. Zhang, *Cryst. Growth Des.* **2012**, *12*, 1808.

[18] S. Chen, R.-Q. Fan, C.-F. Sun, P. Wang, Y.-L. Yang, Q. Su, Y. Mu, *Cryst. Growth Des.* **2012**, *12*, 1337.

[19] a) E. J. McLaurin, L. R. Bradshaw, D. R. Gamelin, *Chem. Mater.* **2013**, *25*, 1283; b) X.-C. Shan, F.-L. Jiang, D.-Q. Yuan, H.-B. Zhang, M.-Y. Wu, L. Chen, J. Wei, S.-Q. Zhang, J. Pan, M.-C. Hong, *Chem. Sci.* **2013**, *4*, 1484.

[20] a) A. Cadiau, C. D. Brites, P. M. Costa, R. A. Ferreira, J. A. Rocha, L. D. Carlos, *ACS Nano* **2013**, *7*, 7213; b) C. D. Brites, P. P. Lima, N. J. Silva, A. Millan, V. S. Amaral, F. Palacio, L. D. Carlos, *Nanoscale* **2012**, *4*, 4799.

[21] a) Y. Cui, H. Xu, Y. Yue, Z. Guo, J. Yu, Z. Chen, J. Gao, Y. Yang, G. Qian, B. Chen, *J. Am. Chem. Soc.* **2012**, *134*, 3979; b) Y. Cui, W. Zou, R. Song, J. Yu, W. Zhang, Y. Yang, G. Qian, *Chem. Commun.* **2014**, *50*, 719; c) X. Rao, T. Song, J. Gao, Y. Cui, Y. Yang, C. Wu, B. Chen, G. Qian, *J. Am. Chem. Soc.* **2013**, *135*, 15559.

[22] M. Xiao, P. R. Selvin, *J. Am. Chem. Soc.* **2001**, *123*, 7067.

[23] F. Auzel, *Chem. Rev.* **2004**, *104*, 139.